J Am Oil Chem Soc (2007) 84:877–884
DOI 10.1007/s11746-007-1114-9

ORIGINAL PAPER

Effect of Ultrasonication on Droplet Size in Biodiesel Mixtures

Peng Wu · Ying Yang · José A. Colucci · Eric A. Grulke

Received: 12 April 2007 / Revised: 16 July 2007 / Accepted: 18 July 2007 / Published online: 7 August 2007

Abstract Biodiesel fuels have become more attractive recently because of their environmental benefits and cost competitiveness compared to diesel fuel. Many processing improvements have been proposed to increase the conversion rates and the yields of vegetable oil in order to lower production costs and improve biodiesel product quality. In conventional biodiesel production chemistries, alkaline transesterifications of alcohol/oil dispersions should occur primarily near the interface. Ultrasonic mixing has already been shown to increase overall conversion rates for alcohol/vegetable oil mixtures. Our data show that ultrasonic mixing produced smaller droplet sizes than conventional agitation, leading to more interfacial area for the reaction to occur. Droplet size distributions have been measured for conventional impeller and ultrasonic mixing systems using methanol/soybean oil as a model system. The dispersions were stabilized by surfactant in order to obtain droplet size distribution for mixture samples. Ultrasonic mixing produced dispersions with average droplet sizes 42% smaller than those generated using standard impellers.

Keywords Droplet size distribution · Dispersions · Emulsion stability · Mechanical agitator · Ultrasound

P. Wu · Y. Yang · E. A. Grulke (✉)
Department of Chemical and Materials Engineering,
University of Kentucky, 359 RG Anderson Building,
Lexington, KY 40506-0503, USA
e-mail: egrulke@engr.uky.edu

J. A. Colucci
Department of Chemical Engineering,
University of Puerto Rico, Mayagüez Campus,
Mayagüez, PR 00681, USA

Introduction

Biodiesel Processes

Biodiesel, a mixture of alcohol esters of long chain fatty acids, is biodegradable and non-toxic. It is a diesel fuel supplement or alternative due to its environmental benefits [1]. Biodiesel is made by transesterification of vegetable oils, fats and greases with short chain alcohols. Acids, bases or enzymes can be used as catalysts. Acid catalysis is preferred if there are significant quantities of free fatty acids in the feed stock, but the conversion rate is low and high levels of alcohols are needed to force the reaction equilibrium toward the transesterified products [2]. Ester conversions of 95.1 and 99.7% [3] have been reported. Lipase can catalyze 98.4% conversion to biodiesel esters [3] but is expensive. Soybean oil is the most common source for biodiesel production because the cetane number for biodiesel made from soybean oil is higher than other oils [3]. Due to the low cost of methanol and the high rates of base-catalyzed transesterifications, most commercial biodiesel is made by the alkali-catalyzed reaction of soybean oil with methanol.

Alkali Transesterification

Alkali-catalyzed transesterification requires a low molar ratio of alcohol to oil (6:1) plus low catalyst levels, and achieves high conversions at low batch times [4]. There are several disadvantages of this process. Feedstocks with high levels of free fatty acids (particularly recycled oils and greases) tend to produce soap byproducts with the alkali catalysts, reducing conversions, making separations more

difficult, and leading to lower purity methyl esters and glycerol [1, 5]. The presence of water in the oils and feedstocks also induces soap formation. The glycerol co-product is recovered by settling or centrifugation, and needs to be sold for good process economics. Biodiesel standards are issued or under review in Europe and in the US [6]. The ASTM standards pertinent to biodiesel include the water and sediment levels (ASTM 1796, 0.050 vol % max), acid number (ASTM 664, 0.80 mg KOH/g max), free glycerol (GC, 0.20 wt % max) and total glycerol (GC, 0.40 wt % max).

The volume ratios of biodiesel reactants are linked to various molar ratios of alcohol/fatty acid content. In general, the alcohol/triglyceride molar ratio should be 3:1 or greater so that all glycerol segments can be replaced by alcohol groups. Because of the density differences between the two phases and their interfacial energy, methanol/soybean oil dispersions are unstable and coalesce in the absence of agitation. The rate of coalescence is important both during biodiesel synthesis and downstream separation of the reaction products.

Effects of Ultrasonic Mixing on Droplet Formation and Reaction Rates

Cavitation induced by ultrasound has been shown to have significant effects on liquid phase reactions. In a semi-batch reactor, Monnier and coworkers [7] showed that dissipated power, rather than power per unit mass, correlated with reaction rates for parallel competing reactions. Characteristic mixing times could be as short as 0.005 s [8], and the flow of the liquid through the ultrasonication zone was critical to the process result. This last finding has implications for scale-up and modifications of biodiesel processes. Injection of reacting systems into the volume near the sonication horn is critical for the best results [9]. Acoustic cavitation could help generate small droplets, and large interfacial areas if the ultrasonication device is placed near the liquid–liquid interface in a two phase reaction system [10, 11].

Research Objectives

This work compares the droplet size distributions of methanol/soybean oil dispersions generated by impeller and ultrasonic mixing. The droplet distributions were stabilized using a dispersant to slow coalescence so that size distributions could be measured by light scattering techniques.

Theory

Rate-Limiting Mechanisms

Alkali-catalyzed transesterification of triglycerides with alcohols are known to be consecutive reversible reactions. Esters are released sequentially from the triglyceride, leaving three moles of ester and one mole of glycerol. Eckey [12] developed a detailed reaction mechanism. The actual catalyst is thought to be the alkoxide formed when the base is added to the alcohol [13]. The alkoxide and the alkali are not very soluble in the oil phase, and the reaction is known to be rate-limited by the interfacial area. In this sense, the reaction mechanism is similar to other two phase reaction systems for oils, such as epoxidation of soybean oil with peroxide and an acid catalyst [14].

Biodiesel production from seed oils has been improved with the application of ultrasonication. Stavarache et al. [4] reported that, with high frequency ultrasound (40 kHz), the transesterification process proceeded quickly and increased biodiesel yield. Colucci [15] showed that ultrasonication increased the apparent rate constants of alkaline transesterification.

Effect of Impeller Speed on Particle Size Distribution

In liquid–liquid systems, the energy input from the impeller can be related to droplet size. In general, high shear and turbulent flow conditions are needed for the impeller to generate small droplets. The mechanical energy required to create turbulence depends on both geometry of the vessel and impeller and physical properties of the liquids.

When the height of the liquids and the diameter of the vessel are related to the diameter of the impeller, the power consumption, P, can be expressed by following equation:

$$P = C\rho N^3 d^5 \left(\frac{\rho N d^2}{\mu}\right)^x \left(\frac{N^2 d}{g}\right)^y \quad (1)$$

in which C is a constant, ρ and μ are the density and viscosity of the liquid, N is the speed of the impeller, d is the diameter of the impeller and g is the gravitational acceleration.

According to Eq. (1), the power number $N_P (N_P = P/\rho N^3 d^5)$ can be expressed as a function of two dimensionless number, Reynolds number $(\mathrm{Re} = \rho N d^2/\mu)$ and Froude number $(Fr = N^2 d/g)$.

$$N_P = f(\mathrm{Re}, Fr) \quad (2)$$

The Reynolds number and Froude number represent the ratios of applied force to viscous force and gravitational

force, respectively, and both relate to the speed of the impeller. The power number should relate to droplet size.

When phase separation occurs in a liquid mixing process, another dimensionless number, Weber number ($We = \rho N^2 d^3/\sigma$, σ: interfacial tension of two liquid phases) becomes important and affects the critical power consumption to reach turbulence in the vessel. Therefore, the power number should be expressed as:

$$N_P = f(\mathrm{Re}, Fr, We) \tag{3}$$

Critical Agitator Speed

In a mixture of two immiscible liquids, there is a critical agitator speed, N_c, at which a separated immiscible layer disappears [16]. When the impeller is composed of four blades with the diameter of the blades set at 1/3 of the tank diameter, the ratio of the width of the baffles to the diameter of the container is 0.10 and the distance between the impeller and the bottom of the tank is 1/2 of the diameter of the tank, N_c can be calculated by the empirical equation:

$$N_c = KD^{-2/3}\left(\frac{\mu_c}{\rho_c}\right)^{1/9}\left(\frac{\rho_c - \rho_d}{\rho_c}\right)^{0.26} \tag{4}$$

in which K is a proportional coefficient, ρ_c and ρ_d are the densities of the continuous and dispersed phases, respectively, μ_c is the viscosity of the continuous phase, and D is the vessel diameter.

Experimental Procedures

Materials

Technical grade soybean oil was purchased from Cargill Industrial Oils and Lubricants and used without further purification. Methanol (HPLC grade) was supplied by EMD Chemicals Inc., Decaglycerol mono-oleate (MO750; CAS Reg #79665-93-3) was kindly provided by Sakamoto Yakuhin Kogyo Co., Ltd., Osaka. Sorbitan monostearate (Span 60; CAS Reg #1338-41-6) was purchased from Alfa Aesar and sorbitan monooleate (Span 80; CAS Reg #1338-43-8) was purchased from Aldrich Chemical.

Centrifugation Assay

Centrifugation assays were used to determine the relative effectiveness of several surfactants for slowing the coalescence process. Emulsions were prepared with 10 mL soybean oil, 1.3 mL methanol (molar ratio of methanol to oil was 3:1; the volume fraction of methanol was 0.115), one droplet of food dye and 0.1 wt % dispersant (sorbitan monostearate, sorbitan monooleate or decaglycerol monooleate, separately). After stirring at 300 rpm for 10 min, 7 mL of each emulsion was placed in a 8-mL glass tube and centrifuged for 1 min with an IEC Centra-4B centrifuge (International Equipment Company) at 300 rpm at room temperature (23 °C). Phase-separated samples had two layers with methanol in the upper layer.

Dispersant Stabilization

Soybean oil, methanol (molar ratio 1:1) and 0.1% (weight percent) MO750 were mixed in a 1 gallon tank (D_{inside} = 17 cm, H = 20 cm, liquid fill level = 10 cm, impeller blade 4 cm off the tank bottom, horn near the impeller) with four baffles (width = 1.7 cm) inside and an impeller. The ultrasonication was done with a UP400S processor with an operating frequency of 24 kHz (Hielscher Ultrasonics GmbH, Germany). The diameter of the horn is 1.5 cm. The mechanical agitator was a Lightnin Bench Biomixer with an adjustable speed up to 1,800 rpm. The impeller was a flat blade turbine with six blades (diameter = 5 cm, height of the blade/diameter = 0.2). The input power both of ultrasonicator and impeller can be measured directly with a power meter (P4400 KILL A WATT™).

Measurement of Interfacial Tension

Interfacial tensions were measured at 23 °C using the pendant droplet method with a contact angle measuring instrument (Droplet shape analysis System DAS 10, Krüse, USA). Every sample was measured at least six times to ensure reproducibility. The interfacial tension of methanol/soybean oil was 3.82 ± 0.12 mN/m. The interfacial tension of methanol with 0.1 wt % MO750/soybean oil was 3.44 ± 0.02 mN/m.

Measurement of Droplet Size Distribution

Mixtures of methanol/soybean oil (1:1 by molar ratio and 0.04 volume fraction) were dispersed either by agitation in a conventional stirred tank or by ultrasonication. Higher volume fractions of methanol led to turbidity in the dispersion that prevented reproducible droplet size measurements. When the mixing process was completed, 3 mL of the emulsion was removed for droplet size measurement. Size distributions were determined by photon correlation spectroscopy of quasi-elastically scattered light using a 90 plus/BI-MAS particle size analyzer (Brookhaven Instruments Corporation, USA). Three separately prepared samples were measured and the mean value was used.

Results and Discussion

Stabilization of Methanol/Soybean Oil Dispersions

Photon correlation spectroscopy for determining particle size distributions (PSDs) requires that signals are collected for a period of minutes (the preferred time is determined by the quality of the data). Coalescence of methanol droplets in the dispersions started immediately as the sample was being removed from the vessel, so that PSD measurements were not reproducible. Therefore, a stabilizing agent or dispersant was sought that could be added to the dispersion to slow the coalescence phenomenon.

Three dispersants were tested: sorbitan monostearate (Span 60), sorbitan monooleate (Span 80) and decaglycerol monooleate (MO750) (the chemical structures of these stabilizers are shown in Scheme 1). The stabilization of four methanol/soybean oil mixtures: without surfactant (blank), with Span 60, with Span 80 and with MO750 was tested using the centrifugation method. After centrifuging at 300 rpm for 1 min, the blank (control) sample containing no dispersant quickly phase separated. The coalescence kinetics was slow for the two Span samples, and very slow for the MO750 dispersant. The MO750 was chosen as the best of this set to stabilize the droplets for size distribution measurements.

The hydrophilic–lipophilic balance (HLB) of a surfactant is an empirical parameter used to predict the emulsion type (water in oil or oil in water). The HLB values for the surfactants were: Span 60 4.7; Span 80 4.3; and MO750 12.9. The Bancroft rule states that the phase in which a surfactant is more soluble constitutes the continuous phase. MO750 having the higher HLB value, is expected to be more polar, and therefore, more soluble in the methanol phase. If the Bancroft rule would apply in this mixture, the methanol would form the continuous phase. Prior research with the MO750 surfactant in alcohol/oil mixtures has shown that the Bancroft rule does not apply, and suggests that stratification theory describes the stabilization that occurs in the interphase region [17]. For example, Xu et al. [17] reported that the interfacial tension of 95% ethanol/oil mixtures changes slightly with the addition of MO750 (from 2.57 to 1.76 mN/m). This surfactant is not particularly surface active, but is thought to form aggregates in the interfacial film. These aggregates stabilize the interphase region and arrest the coalescence of droplets. Our measurements of the interfacial tension of methanol/soybean oil, using the pendant droplet technique, show a similar slight change in this parameter (from 3.82 ± 0.12 mN/m for the neat interface to 3.44 ± 0.02 mN/m with MO750 added). Therefore, we expect that MO750 stabilizes the methanol droplets via a stratification mechanism as well.

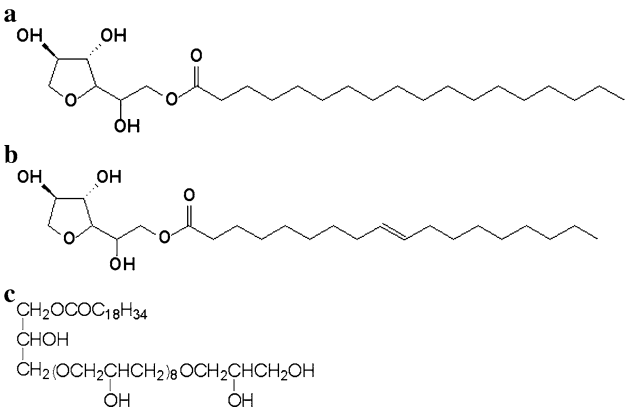

Scheme 1 Chemical structures of **a** Span 60, **b** Span 80, and **c** MO750

Settling Experiment to Verify Droplet Instability

Some dispersants might generate stable emulsions with droplets sizes set by the dispersant system and not the mixing process. Therefore, it was necessary to demonstrate that the dispersant simply slowed the kinetics of coalescence, but did not prevent the process. Water-soluble food dye was added in each emulsion so that phase separation could be clearly observed visually: the dye migrated to the methanol phase instead of the oil phase. In the system of methanol/MO750/soybean oil, after 2 days of settling, methanol droplets coalescence with the MO750 dispersant which shows that it is a thermodynamically unstable emulsion. Phase separation was nearly complete, which indicated that no thermodynamically stable emulsion forms in the methanol/soybean oil system with the additive of MO750. The MO750 dispersant was used to stabilize droplets for impeller and ultrasonic mixing tests.

Minimum Critical Agitator Speed

As shown in Eq. 4, the critical agitator speed needed for droplet dispersion sets the lower limit for practical agitation for biodiesel processes. The following parameter values were used to estimate this speed: K was taken as 750 for the agitation in center of the vessel, ρ_c was 920 kg/m^3 , ρ_d was 791 kg/m^3, μ_c was 0.05 Pa s, and D was 17 cm. The minimum critical agitator speed was N_c = 493 rpm. Dispersion experiments performed at 500 rpm gave droplet size distributions that were not reproducible, a reasonable result considering that Eq. 4 is empirical. Dispersion experiments done at rpm's 10% greater than the N_c estimate ($N > 550$ rpm) gave reproducible results. Figure 1a shows the mean droplet size versus input energy for an impeller speed below the critical minimum value

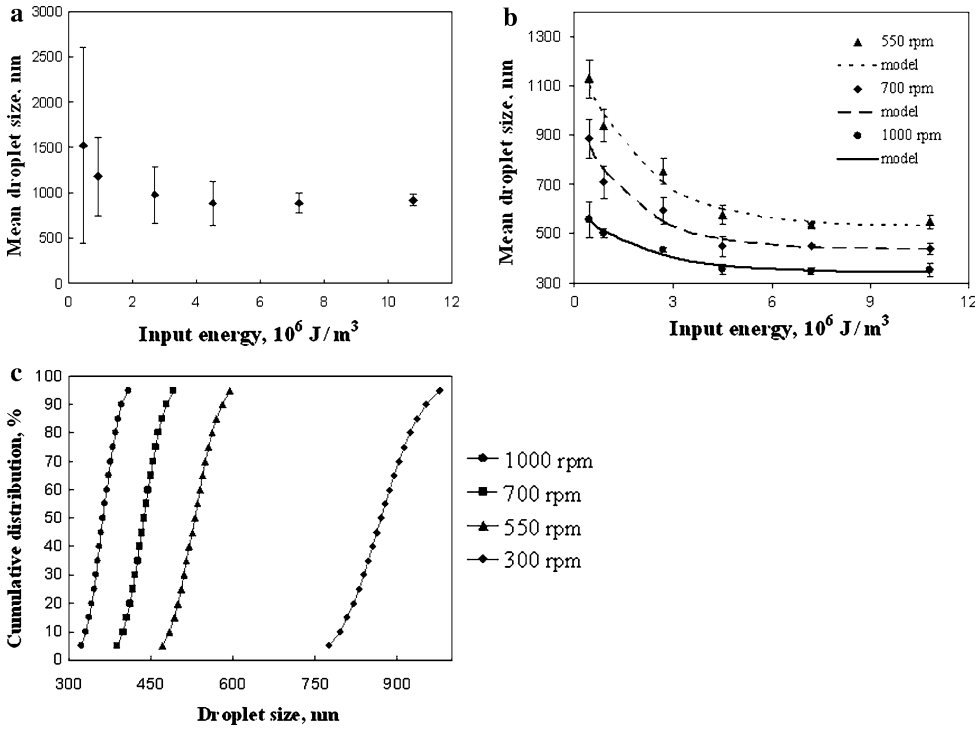

Fig. 1 **a** Mean droplet size versus input energy for an impeller speed below N_c (300 rpm). **b** Mean droplet size versus input energy at three impeller speeds above N_c. The model (*line*) is Eq. 5 fitted to the data. **c** Cumulative droplet size distributions for uniform dispersions

(N = 300 rpm when N_c = 493 rpm). The standard average error of the droplet size measurements is large compared to the mean value for all input energies, and is particularly poor for low input energies (or short mixing times). A steady state mean droplet size is approached for high input energies, but its distribution is quite broad compared to the mixtures at higher impeller speeds (see Fig. 1b).

Equation 4 provided a good estimate for the minimum rpm for reproducible droplet formation in the methanol/soybean oil mixture. Therefore, it might be useful in setting the lower agitation limits for commercial biodiesel plants.

Effect of Impeller Speed on Droplet Size

Figure 1b shows typical mean droplet diameter changes with input energy for three different impeller speeds above the critical agitator speed. In all cases, the droplet size is large initially. With increasing input energy, the droplet size approaches a steady-state value as the breakage and coalescence processes reach a dynamic equilibrium. If the experimental time is used as the independent variable (suggested by Gäbler [18]), the curves have similar shapes. The error bars in Fig. 1b represent one standard deviation (average standard error) from the mean. At higher energy inputs or longer experimental times, the mean droplet sizes approach different steady state values for each impeller speed, with lower speeds yielding larger droplet sizes. In general, the average standard errors are lower for higher speeds and the dispersion is more uniform. At 1,000 rpm, the median methanol droplet diameter is $\sim$350 nm.

An important question for droplet dispersion processes is when has the droplet size distribution approached its steady state value? A simple first order reverse rate equation can be used to model the mean droplet size as a function of time (or input energy). The rate of change in the mean droplet is:

$$-\frac{dD_p}{dE} = k(D_p - D_p^{\min}) \tag{5}$$

where E is the input energy, D_p is mean droplet size, $D_p^{\min}$ is the minimum droplet size, and k is the rate constant. Then

$$D_p = D_p^{\min} + (D_p^{\max} - D_p^{\min}) \cdot e^{-k \cdot E} \tag{6}$$

Equation 6 fits the experimental data very well, as shown by the curves in Fig. 1b. If the condition for steady-state is taken to be when the droplet size is within 5% of its minimum value, the model suggests that this condition is reached when the input energy is $\sim 5 \times 10^6$ J/m^3, which is confirmed by the experimental data. After the droplet size reaches a minimum value, increasing the input energy cannot help to break droplets any further. The data in Fig. 1a, b suggest that steady-state dispersions are reached for input energies greater than 7.2×10^6 J/m^3. At 300 rpm, it took about 12 min to achieve a uniform distribution, while at 1,000 rpm, it took less than 5 min. Both the mean

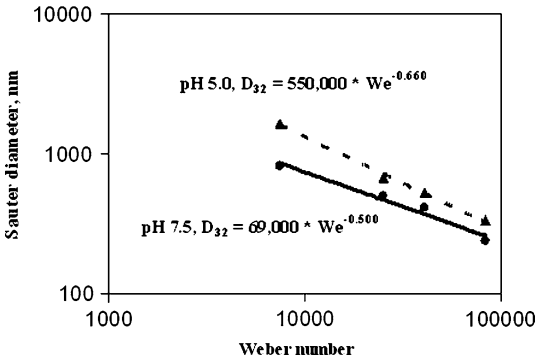

Fig. 2 Sauter mean diameter (D_{32}) versus Weber number. Methanol/soybean oil at pH 5.0 and 7.5

droplet size and the time to reach steady state would be important to biodiesel production.

Figure 1c shows the steady state droplet size distributions for the same input energy (7.2×10^6 J/m^3). Increasing the speed of the impeller shifts the distribution toward smaller droplets and narrows the distribution. At 300 rpm, the droplet distribution is broad and there are very few droplets less than 750 nm. At 550 rpm, most of the droplet sizes range from 450 to 600 nm, while at 1,000 rpm, the droplet sizes range from 320 to 380 nm. These differences represent large changes in the interfacial areas between the four dispersions. Gäbler et al. [18] studied the effect of impeller rpm and phase fraction and pH on an oil-in-water (toluene in water) dispersion. At a constant volume fraction of his dispersion, increasing the impeller speed shifted the particle size distributions to lower mean droplet sizes and narrowed the distributions significantly.

The results for the methanol-in-soybean oil dispersion are consistent with those of Gäbler [18] for a toluene/water dispersion with a toluene volume fraction of 0.05. Some biodiesel researchers have proposed higher methanol/soybean oil ratios, which would result in higher dispersed phase volume fractions. Gäbler et al. [18] showed that increasing the dispersed phase volume fraction from 0.05 to 0.5 increased the mean droplet size and increased the breadth of the size distribution. It seems likely that similar effects would occur in the methanol/soybean oil system at higher methanol volume fractions.

The impeller Weber number is often used for commercial scale-up of liquid–liquid dispersions. It is the ratio of the fluid inertia to surface tension and relates to the formation and coalescence of droplets. The impeller Weber number includes the fluid density, the interfacial energy, the impeller speed and the impeller diameter, and can be used to scale droplet formation with temperature or dispersed phase volume fraction. In general, droplet diameters decrease as the Weber number increases, i.e., coalescence decreases. The Sauter mean diameter, D_{32}, which is based on a surface area average of the droplets, is preferred as the correlated variable. However, some important commercial systems exhibit parabolic behavior between the two variables, which is thought to be caused by increasing coalescence rates [19]. Steady-state droplet diameters for methanol/soybean oil dispersions at different pH values are plotted versus impeller Weber number in Fig. 2. The proportionality between the mean diameter and Weber number is d $\sim We^{-0.50}$ at pH = 7.5. Decreasing the pH value (pH = 5) increased the mean droplet size and decreased the Weber number exponent to −0.66. Gäbler [18] found that, in toluene-water system, increasing the pH value increases the exponent which is quite similar to the empirical correlations in Fig. 2. It is clear that by adjusting the pH value of the systems, the speed of coalescence processes may be changed both in biodiesel reaction systems as well as downstream processing to separate the liquid product phases.

Effect of Ultrasonication on Particle Size Distribution

The mean droplet size of the methanol phase decreased as the input energy increased (Fig. 3a). The ultrasonic horn expends much more energy per unit volume to achieve the steady-state mean droplet size for the mixture. There are several factors that impact the higher energy input. The

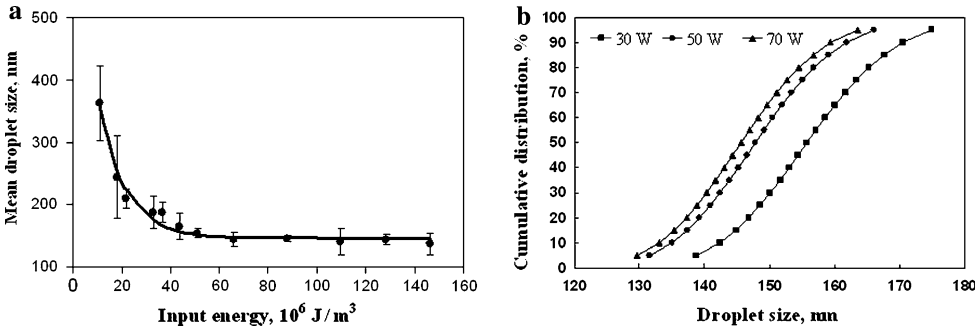

Fig. 3 **a** Mean droplet size versus input energy for ultrasonication. **b** Cumulative droplet size distributions for three ultrasonication power settings. Input energy = 90×10^6 J/m^3

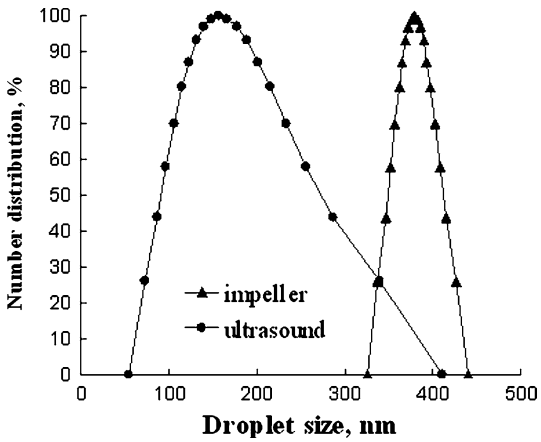

Fig. 4 Comparison of differential droplet distributions for impeller and ultrasonic agitation. Input energy = 10.8×10^6 J/m^3

cavitation zone of the wand is small, the wand is not particularly efficient in moving fluid throughout the vessel volume, and the droplet sizes are much smaller than those achieved with a conventional impeller. In contrast to the data in Fig. 1b, there are large standard deviations in the mean droplet size at lower energy inputs when ultrasonication is used. However, at input energies greater than 50×10^6 J/m^3, steady-state droplet size distributions were achieved. The minimum droplet size is about 140 nm, which is three times smaller than the droplets obtained with impeller at 1,000 rpm.

With ultrasonic energy, both the time period for sonication and the sonication power can be varied. Figure 3b shows the effects of power intensity on the droplet size distribution at a specific input energy level, 90×10^6 J/m^3. The shapes of these three curves under different power intensities are similar. At an intensity of 30 W, the mean droplet size is 156 nm. At intensities of 50 and 70 W, the mean droplet sizes are 148 and 146 nm, respectively. The difference of mean droplet size between 50 and 70 W is modest (2 nm), which suggests that increasing the intensity above 70 W would give little reduction in the mean droplet size.

Comparison Between Impeller and Ultrasound Mixing

Figure 4 compares the droplet size distributions for the impeller (1,000 rpm) and ultrasonication (30 W) at the same input energies. The mean droplet size for the impeller agitation is a factor of 2.4 times larger than that of the ultrasonication system. The broad particle size distribution is probably due to the short duration of ultrasound agitation with no pre-mixing treatment of the mixture.

Ultrasound pressure waves alternately compress and stretch the molecular spacing of the liquid, and can generate gas and vapor bubbles. The continuous generation and collapse of cavitation bubbles in the liquid breaks large droplets into small ones. Compared to ultrasound, impellers generate turbulent shear flows which make droplets. Ultrasonication often results in smaller droplets than turbulent shear flows.

Compton and coworkers [20] have previously derived rate expressions for a liquid–liquid interfacial reaction system for copper extraction from an aqueous solution into an organic liquid, assuming a first order reaction with species B at the interface. If mixing in both the dispersed and continuous phases is good, then the bulk concentrations of each phase will be near that of the interfaces and the change in concentration with time is

$$-\frac{\mathrm{d}[B]}{\mathrm{d}t} = \frac{k4\pi r^2}{V} N[B]$$

where V is the volume of the dispersed phase, r is the droplet radius and N is the total number of particles. The effective rate constant for the process should correspond to the surface rate constant by

$$K_{eff}(r) = \frac{k4\pi r^2}{V} N = \frac{kN}{V} S_{droplet,average}$$

Therefore, the effective rate constant for the ultrasonication system could be as much as six times that of the conventional agitation system. Combining conventional agitation systems to move fluid through the vessel and through the ultrasonication zone might provide further reductions in the mean droplet size and improve the energy efficiency of a combined agitation system (impeller + ultrasonication).

Mechanical dispersion of the methanol/soybean oil mixture by both impellers and ultrasonication can lead to mean droplet sizes less than 1 μm. Increases in impeller speed or in ultrasonic wand power lead to smaller mean droplet sizes. The mean droplet size correlates with Weber number, and seems sensitive to the pH of the system. Ultrasonication can result in mean droplet sizes much lower than those generated by conventional agitation, and can be a more powerful tool in breaking methanol into small droplets.

Acknowledgments This research was supported by the Kentucky Soybean Promotion Board and the Center for Plant Biotechnology Research.

References

1. Fukuda H, Kondo A, Noda H (2001) Biodiesel fuel production by transesterification of oils. J Biosci Bioeng 92(5):405–416
2. Freedman B, Pryde EH, Mounts TL (1984) Variables affecting the yields of fatty esters from transesterified vegetable oils. J Am Oil Chem Soc 61(10):1638–1643

3. Shimada Y, Watanabe Y, Samukawa T, Sugihara A, Noda H, Fukuda H, Tominaga Y (1999) Conversion of vegetable oil to biodiesel using immobilized *Candida antarctica* lipase. J Am Oil Chem Soc 76(7):789–793
4. Stavarache C, Vinatoru M, Nishimura R, Maeda Y (2003) Conversion of vegetable oil to biodiesel using ultrasonic irradiation. Chem Lett 32(8):716–717
5. Ma F, Hanna MA (1999) Biodiesel production: a review. Bioresour Technol 70:1–15
6. Knothe G, Dunn RO, Bagby MO (1997) Biodiesel: the use of vegetable oils and their derivatives as alternative diesel fuels. ACS Symposium Series, 666 (Fuels and Chemicals from Biomass): 172–208
7. Monnier H, Wilhelm AM, Delmas H (1999) The influence of ultrasound on micromixing in a semi-batch reactor. Chem Eng Sci 54(13–14):2953–2961
8. Monnier H, Wilhelm AM, Delmas H (2000) Effects of ultrasound on micromixing in flow cell. Chem Eng Sci 55(19): 4009–4020
9. Monnier H, Wilhelm AM, Delmas H (1999) Influence of ultrasound on mixing on the molecular scale for water and viscous liquids. Ultrason Sonochem 6(1–2):67–74
10. Bondy C, Sollner K (1935) Mechanism of emulsification by ultrasonic waves. Trans Faraday Soc 31: 835–843
11. Sivakumar M, Senthilkumar P, Majumdar S, Pandit AB (2002) Ultrasound mediated alkaline hydrolysis of methyl benzoate—reinvestigation with crucial parameters. Ultrason Sonochem 9(1): 25–30
12. Eckey EW (1956) Esterification and interesterification. J Am Oil Chem Soc 33:575–579
13. Sridharan R, Mathai IM (1974) Transesterification reactions. J Sci Ind Res 33: 178–187
14. Rangarajan B, Havey A, Grulke EA, Culnan PD (1995) Kinetic parameters of a two-phase model for in situ epoxidation of soybean oil. J Am Oil Chem Soc 72(10):1161–1169
15. Colucci JA, Borrero EE, Alape F (2005) Biodiesel from an alkaline transesterification reaction of soybean oil using ultrasonic mixing. J Am Oil Chem Soc 82(7):525–530
16. Shinji N (1975) Mixing: principles and applications, 1st edn. Wiley, New York
17. Xu Q, Nakajima M, Nabetani H, Ichikawa S, Liu X (2001) Effect of the dispersion behavior of a nonionic surfactant on surface activity and emulsion stability. J. Colloid Interface Sci 242: 443–449
18. Gabler A, Wegener M, Paschedag AR, Kraume M (2006) The effect of pH on experimental and simulation results of transient distributions in stirred liquid–liquid dispersions. Chem Eng Sci 61: 3018–3024
19. Johnson GR (1980) Effects of agitation during VCM suspension polymerization. J Vinyl Technol 2(3):138–140
20. Banks CE, Klymenko OV, Compton RG (2003) Liquid–liquid processes and kinetics in acoustically emulsified media. Phys Chem Chem Phys 5(8):1652–1656